Mechanics of Advanced Composite Structures

Journal homepage: https://macs.semnan.ac.ir/

Semnan University

ISSN: 2423-7043

Research Article

Parametric Investigation of Particle Movements in Ultrasonic Levitation Process Using Piezoelectric Materials

Mohammadreza Sheakholeslami [a*], Davood Dehghani [a], Ali Jabbari [a], Hamid Abdi [b], Siamak Mazdak [a], Simone Cinquemani [c], Abbas Amoochi [a]

[a] *Department of Mechanical Engineering, Faculty of Engineering, Arak University, 38156-8-8349, Arak, Iran*

[b] *School of Engineering, Deakin University, Waurn Ponds, VIC 3217, Australia.*

[a] *Dept. Mechanical Engineering, Politecnico di Milano, Via La Masa 1, 20156, Milan, Italy.*

ARTICLE INFO

Article history:

Received: 2023-10-19
Revised: 2024-03-22
Accepted: 2024-05-12

Keywords:

Ultrasonic levitation,
Piezoelectric transducers,
Distance between transducer and reflector,
Electric Potential,
Finite element method.

ABSTRACT

Using ultrasonic waves to levitate particles is ultrasonic levitation, and it has potential applications in various fields such as micromaterial handling, medicine, and material characterization. For many of these applications, the behavior of the levitated particles during the levitation time is critical, including movements of the particle at a levitated point. Electrical potential and the distance between the transducer and reflector are two main parameters affecting the movement of the levitated particles. In this paper, a second-order linear model considering the effect of these parameters was presented to predict particle movement based on numerical results. In the modeling part, a 2D COMSOL dimensional axis-symmetric finite element model has been used to simulate ultrasonic levitation. Experimental tests have been performed and used to validate the model. The results in this report could help to understand the main factors in the movement of the levitated particle and develop methodologies for particle stabilization.

1. Introduction

Ultrasonic levitation is a process of using ultrasonic waves to levitate particles. The levitation system consists of an ultrasonic transducer and a reflector. An ultrasonic transducer can be used instead of a reflector. If the distance between the piezoelectric transducer and reflector is properly adjusted, the superposition of the original and the reflected waves will create static low-pressure and high-pressure regions, which are alluded to as node and anti-node. The interference between waves generated from the piezoelectric transducer and the reflected wave from the reflector (or generated from the other transducer) will create additional forces on the particles that levitate them.

In addition to the ultrasound levitation mechanism, there are other methods such as magnetic[1], electromagnetic[2], superconductor [3, 4], and optical levitation[5]. Particle levitation has been used in the pharmacy[6], medicine[7], Chemistry[8], Physics[9] and engineering[10] applications. The main limitation of non-

* Corresponding author. Tel.: +98-86-32625722; Fax: +988632774031
E-mail address: m-sheykholeslami@araku.ac.ir

Cite this article as:
Mohammadi, A. and Mahdi-Nia, M., 2025. Title of article. *Mechanics of Advanced Composite Structures*, 12(1), pp. xx-xx
https://doi.org/10.22075/MACS.2024.39315.2050

ultrasound levitation methods is that the levitation depends on the material properties of the particles. Therefore, ultrasonic levitation is independent of the material properties, which makes it more applicable to a wider range of materials and applications. Additionally, ultrasonic levitation provides non-contact movement of particles, which makes it suitable for microassembly.

Within the literature on particle levitation, Gor'kov[11] presented analytical modeling of spherical particle force in the ultrasonic levitation field. It was shown that the viscosity of the acoustic levitation medium and the thermal condition are the main factors in ultrasonic levitation when the particle size is small enough compared with the wavelength. Xie and Wei [12]studied single-axis ultrasonic levitation and enhanced the capability of this method by using the curving surface reflector. Kozuka et al.[13] developed an acoustical particle manipulation method based on phase change of acoustic waves. Henrik Bruus [14] reviewed the fundamentals of the ultrasound acoustophoresis phenomena and the propagation of waves. Zhao and Wallaschek[15] presented a method to levitate a large planner object. The levitated disc also played a reflector role in this method. Baer et al.[16] used a concave shape for the radiating surface and reflector and improved the stabilization of the levitated particle based on it. A stabilization analysis of the new and conventional designs of the ultrasonic levitating device was also conducted. However, there is no discussion about the effect of levitating parameters, such as input voltage, on particle stability. Andrade et al.[17] used a symmetrical array with three ultrasonic transducers to levitate a solid sphere that was 3.6 times larger than the wavelength. Li et al.[18]improved the load capability of near field zone in ultrasonic levitation by adding a groove on the reflector surface. Keremer et al.[9] presented a new method for measuring the viscosity of a fluid under high pressure using ultrasonic levitation. This method resulted in a shorter measurement time compared to the conventional methods. Andrade et al.[19] demonstrated that levitation particle movement can be controlled by changing the distance between the reflector and the transducer at a constant frequency. Andrade et al.[20] showed the effect of drop shape on the resonance behavior of the device and droplet stability. Hasegawa and Murata [21] not only illustrated that levitated droplets exhibit the lowest displacement amplitude at the third pressure node but also reported that the oscillation of droplets in the acoustic field in the vertical direction is considerably smaller than that in the horizontal direction. Argyris et al. [22] noticed that the deformation of an acoustically levitated droplet is influenced by its surface tension. So, they suggested a machine learning algorithm that can obtain the surface tension based on droplet dynamics analysis. Cancino-Jaque et al. [23] maximize the droplet diameter (6.82 mm) that can be levitated in an ultrasonic field by setting the range for the maximum sound pressure level and optimizing the levitation conditions.

The levitated particle stability is an essential subject in many applications of ultrasonic levitation. Particularly, the estimation of particle behavior in the transient region has a strong potential in the applications of ultrasonic levitation in material recognition and evaluation. According to the literature, there is no comprehensive information about this topic. In this paper, a second-order parametric model is presented based on the numerical study to study the effect of input voltage and distance between the transducer and the reflector on the movement of levitated particles. The benefit of this model is ease of use in different applications of evaluating and controlling particles. COMSOL Multiphysics software was used for the numerical simulation. The numerical study consists of the piezoelectric, acoustic, modal, harmonic, and particle tracing physics in COMSOL. Numerical results were validated with the experiments. The contribution of this study is to present a comprehensive model that considers the input voltages and the distance between the transducer and reflector.

2. Ultrasonic Levitation Background

In the theoretical part, the forces involved in the ultrasonic levitation process are gravity w, ultrasonic force Fa, drag force Fd, and buoyancy force Fb. For a spherical particle, the gravity force is obtained from Eq(1) [11].

$$w = \frac{4\pi r^3 \rho g}{3} \tag{1}$$

where r and ρ are the radius and the density, respectively.

Acoustophoretic force from computational fluid dynamics is calculated from Gor'kov's formula Eq(2)[12]. This force is used for the case where particles are significantly smaller than the wavelength of the wave.

$$F_a = -\nabla U \tag{2}$$

where U is the radiation potential and it is obtained from Eq(3) [11].

$$U = 2\pi r^3 \left[\left(\frac{\overline{P_p^2}}{3\rho c^2} \right) f_1 - \left(\frac{\rho \overline{v_p^2}}{2} \right) f_2 \right] \tag{3}$$

where *Pp* is the pressure of the particle, v_p is the particle velocity, *c* is the ultrasound wave velocity in air, and f_1 and f_2 parameters are calculated from Eq(4) and Eq(5) [11].

$$f_1 = 1 - \frac{\rho c^2}{\rho_s c_s^2} \quad (4)$$

$$f_2 = \frac{2(\rho_s - \rho)}{(2\rho_s + \rho)} \quad (5)$$

where c and c_s are the sound speed in levitated medium and levitated particle respectively and ρ_s is the density of the levitated particle.

$$P_b = -\frac{\rho \partial \Phi_{in}}{\partial t} \quad (6)$$

$$v_p(l) = \frac{P_0}{z_f} \sin(kl) \quad (7)$$

$$v_{in} = \nabla \Phi_{in} \quad (8)$$

where Φ_{in} is the velocity potential of the acoustic field.

The drag force Fd is the force that prevents the levitated object from moving in the fluid and it can be determined by Eq(9)[13].

$$F_d = \frac{m_p(u - v)}{\tau_p} \quad (9)$$

where m_p is particle mass, τ_p is particle response velocity, v is particle velocity and u denotes fluid velocity. For the Reynolds number less than 1, the particle response rate for spherical particles in the laminar flow is obtained from Eq (10) [13].

$$\tau_p = \frac{\rho_p d_p^2}{18\mu} \quad (10)$$

where μ is fluid viscosity, ρ_p is the particle density and d_p is the particle diameter.

The buoyancy force follows Archimedes' law and is considered whenever a body is submerged or floated in fluid. The buoyancy force is in the opposite direction of gravity, and it is independent of the shape of the levitated object. The buoyancy force in gases is small and hence could be neglected for the proposed case.

As was described in this section, different complicated forces play a role in the ultrasonic levitation process. So, it is challenging to model particle movement during this process analytically. The numerical method is a suitable alternative for this purpose.

3. Ultrasonic Levitator Design

In this section, the design of an ultrasonic levitator is described. The levitator is composed of a transducer, a reflector, and the support mechanical and electrical/electronic subsystems.

3.1. Transducer and Reflector Specifications

The design procedure and behavior study of a sonic Langevin transducer with magnetostrictive materials was described in [14-18], and the design procedure and behavior study of an ultrasonic transducer with piezoelectric materials was also investigated in [19, 20]. Following the same procedure, a Langevin transducer with a resonance frequency of 20kHz and 2kW nominal power was designed and fabricated. The transducer consists of four main parts, matching, piezoelectric rings, central screw, and backing, all of which have axial symmetry. Figure 1 shows the technical drawing and fabricated picture of the transducer.

Fig. 1. The fabricated transducer

In addition, a wave reflector, with the capability to adjust the distance between the transducer and reflector, was designed and fabricated using aluminum material, and the adjustment mechanism was a screw to change the distance. In addition, even though using a curved reflector could improve stabilization, using a flat reflector occupies less area and provides opportunities for more applications. Hence, a flat reflector was selected for this study.

3.2. Modeling and Numerical Analysis

COMSOL Multiphysics software was used in this study to analyze the levitation process and numerically investigate the behavior of the suspended sample. Because of COMSOL Multiphysics's ability to link several physics, multiphysics problems can be reliably simulated. In other words, in this software, similar to reality, applying a voltage to the piezoelectric changes the length, and length variation creates waves with the desired frequency. This process can be simulated in COMSOL Multiphysics software using solid mechanics, electrostatics, and sound pressure physics.

In the mentioned simulation, after drawing the symmetrical two-dimensional model of the levitation system (Fig.2a) consisting of the transducer with a final cylindrical space with a 90

mm diameter and the reflector (a distance equal to half-wavelength coefficients from the transducer) just like Fig.2b, by applying voltage in electrostatic physics, it is possible to obtain the size change of piezoelectric in solid mechanical physics. In the next step, the mentioned dimension changes cause force distribution in the levitation gap and create a standing wave with the help of acoustic pressure physics.

Finally, by coupling the particle tracing tracking physics, the desired number of particles with the desired properties can be placed in the levitation gap, and by adding gravity force, buoyancy force, and drag force, all the effective factors in the ultrasonic levitation can be investigated in the simulation. The change in the input voltage to the piezoelectrics causes a change in the generated wave and the behavior of the levitated particle.

In the meshing section, the element type was the free triangular element, and the mesh size was equal to 10% of the wavelength according to the mesh-independent study to avoid the effect of mesh size in the results (Fig.2. c).

For the particle movement study, the simulations were repeated for voltage parameters of 200V,300V,400V,500V, and 700V, and distance parameters of (λ/2, λ, and 3λ/2) and five levitated particles. A voltage of more than 700 V is less used in this process due to the complexity of production, safety conditions, and the lack of need for this amount in the levitation of particles. Distances longer than 3λ/2 are rarely used due to wave attenuation. The particle movement along the symmetrical axis of the transducer (z-axis) was recorded for the one-second period and 0.05-second time intervals. The average displacements of the levitated particles were considered a measure of particle movement.

3.3. Experimental Study

The experimental setup (Fig. 2. b) was designed and fabricated to verify numerical results. This setup consisted of a resonance ultrasonic transducer, power supply, adjustable reflector, high-resolution camera, and calibration gauge. An image processing technique was used to measure particle movement. Image processing was calibrated using an accurate calibration gauge (Fig. 2. b). The tests were repeated thrice to increase reliability.

a)

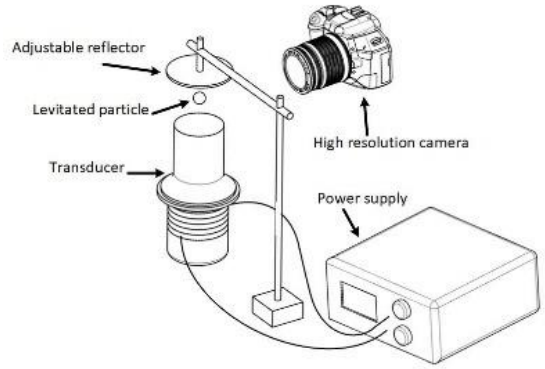

b)

c)

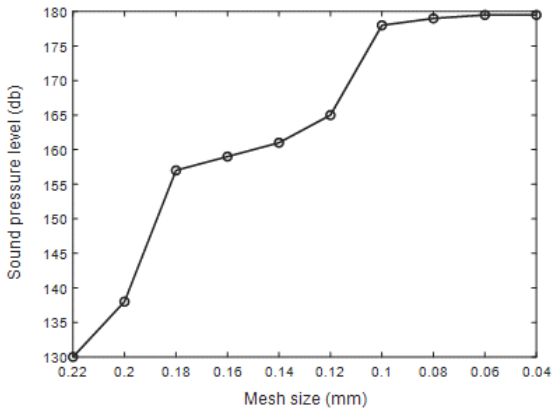

Fig. 2. (a)Schematic of the experimental Setup, (b) Calibration gauge (c) Mesh independence study for the choice of mesh size for FEM analysis

4. Simulation Validation

In the numerical study, to make the conditions uniform in repeating the simulations, the levitation acceptance condition was the levitation of at least one particle of 5 levitated particles. Figure 3 shows the numerical results of particle levitation. Figure 4 shows a comparison between numerical and experimental results. The input voltage was 300V. Figure 4a is associated with half wavelength distance and Figure 4b is related to the wavelength distance between the transducer and the reflector. According to these

Figures, numerical simulation has successfully predicted the particle movement with acceptable accuracy. Both numerical and experimental graphs have the same trends. However, there are more minor oscillations in experimental results. Figure 5 shows the levitated particle movement at successive times in the experiments.

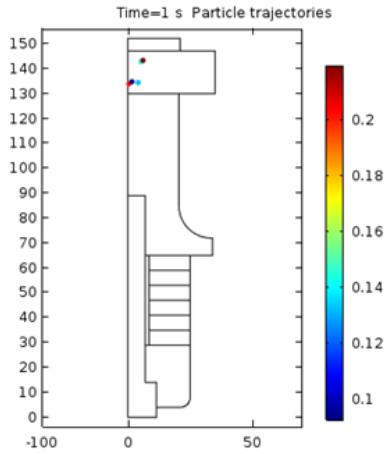

Fig. 3. An example of the particle levitation simulation results obtained from COMSOL software

a)

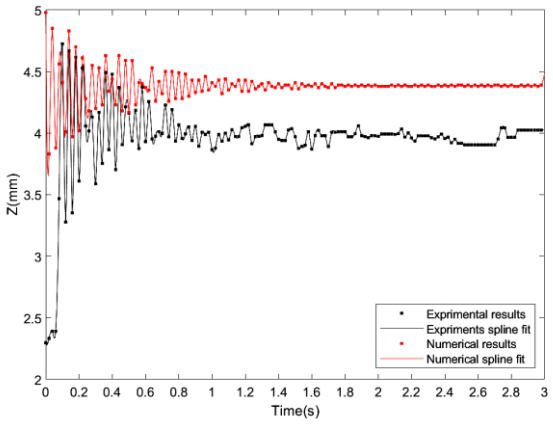

b)

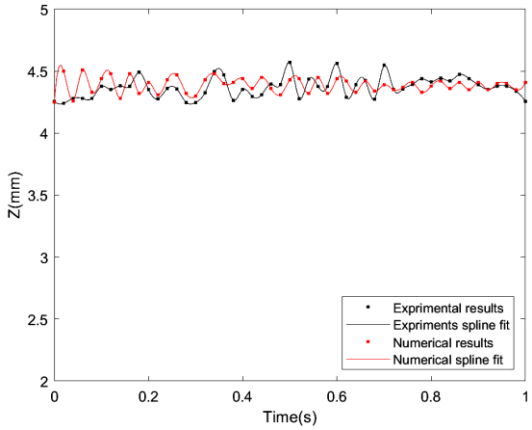

Fig. 4. A comparison study between the numerical and experimental results for the 300v voltage and in (a) λ/2 and (b) λ distances between the transducer and the reflector.

Fig. 5. Movement analysis of the levitated particle in three successive frames of the video recording in the experiments.

5. System identification and modeling

According to the numerical and experimental results, transient and steady-state motion behaviors can be observed for particles in the levitating space. Modeling ontrol of particles. A dynamical transfer function model for levitation was used to model the particle movement based on the numerical results. The second-order parametric model was selected because of its simplicity for use in different applications, where the (a,b,c,d) are the model ((cs+d)/(s^2+as+b)) parameters that have been determined and are the Laplace variable. The second-order model assumption could be further justified by the overshoot and damping behavior of particle movements. Figure 6 shows the system identification process and the corresponding results.

Figure 7 shows the effect of the input voltage on the levitated particle movement in a λ/2 distance between the transducer and the reflector, and Table 1 shows the corresponding model. From this figure, increasing input voltage leads to a decreasing oscillation in particle movement. These phenomena may be coming from increasing input pressure, which results in particles reaching stability in a shorter period. In addition, this situation occurs in a 3λ/2 gap between the transducer and reflector, as shown in the following figures. For a better interpretation of the results, the vertical path is shown in Fig.8(a), and Fig.8(b) represents the pressure distributions at different input voltages in the half-wavelength distances between the transducer and the reflector.

a)

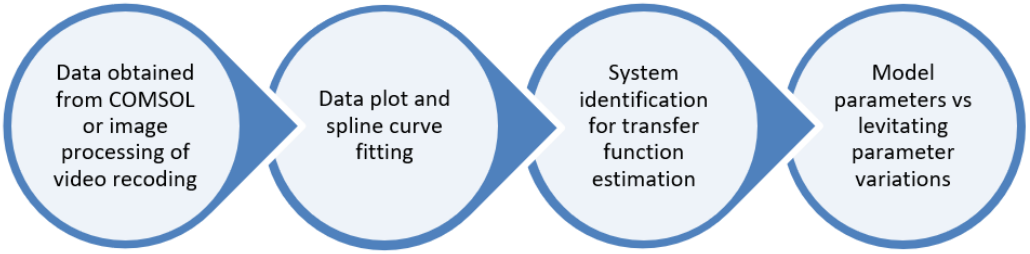

b)

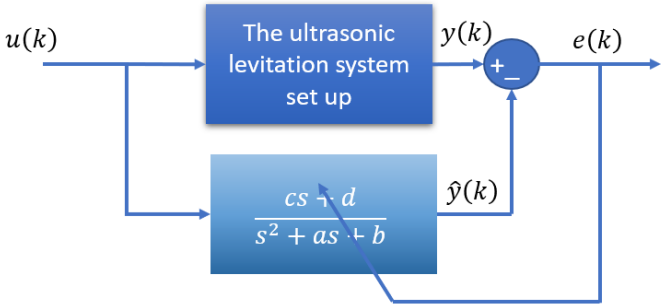

Fig. 6. (a) Data analysis steps, (b) System identification process.

Table 1. Model parameters for λ/2 distance and selected voltage.

	a	b	c	d
200v	503.3011	702.6611	-18.6506	15.4115
300v	84.4753	114.9861	1.2095	1.6802
400v	10.5053	1.8212	0.0601	0.0200
500v	20.1498	40.9881	0.2532	0.3588
700v	1.0863	0.5498	0.0034	0.0034

Transfer function $\frac{cs+d}{s^2+as+b}$

* Corresponding author. Tel.: +98-86-32625722; Fax: +988632774031
E-mail address: m-sheykholeslami@araku.ac.ir

Cite this article as:
Mohammadi, A. and Mahdi-Nia, M., 2025. Title of article. *Mechanics of Advanced Composite Structures*, 12(1), pp. xx-xx
https://doi.org/10.22075/MACS.2024.39315.2050

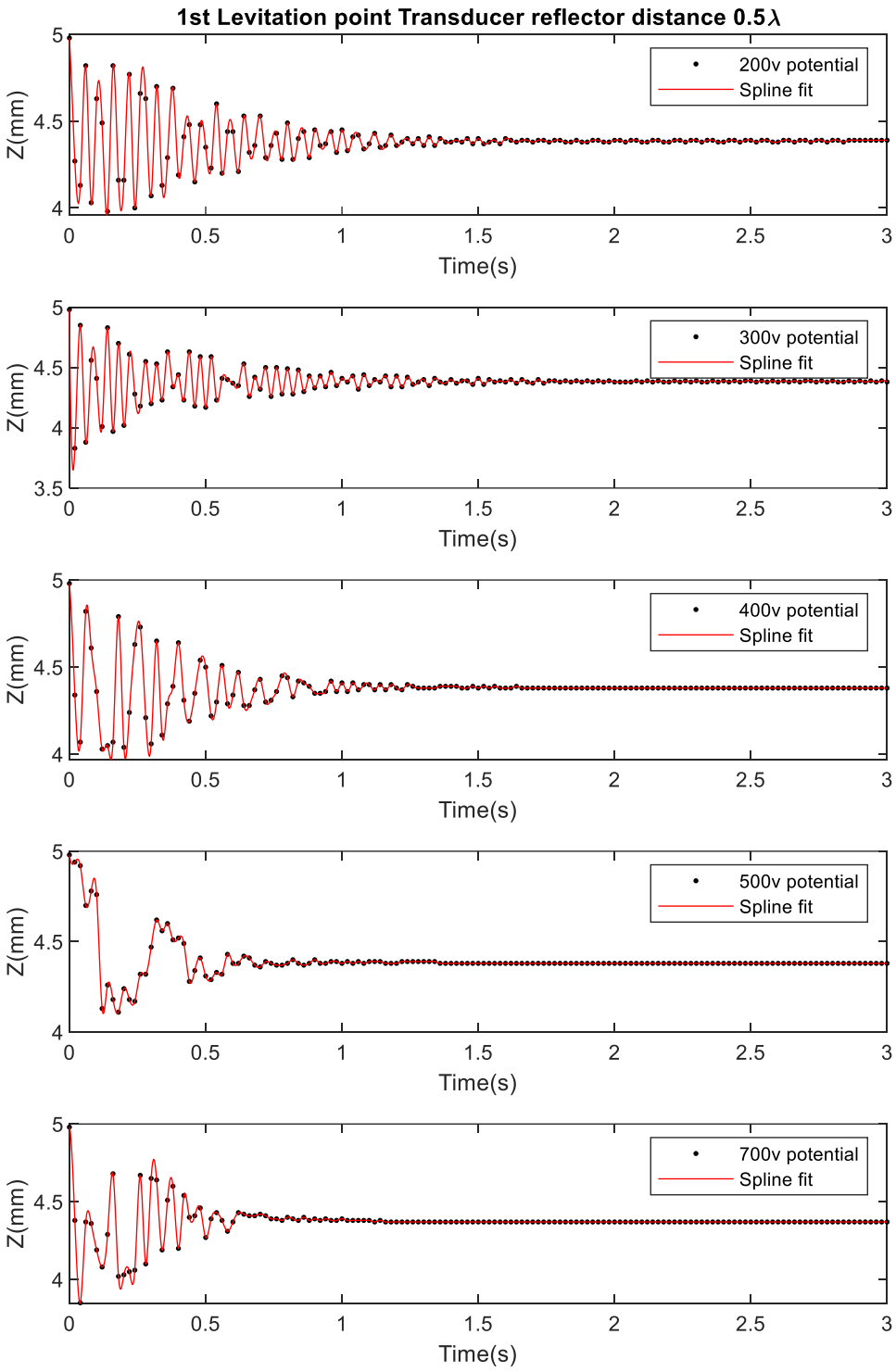

Fig. 7. The particle movement in λ/2 distance between the transducer and the reflector for selected voltages.

a)

b)

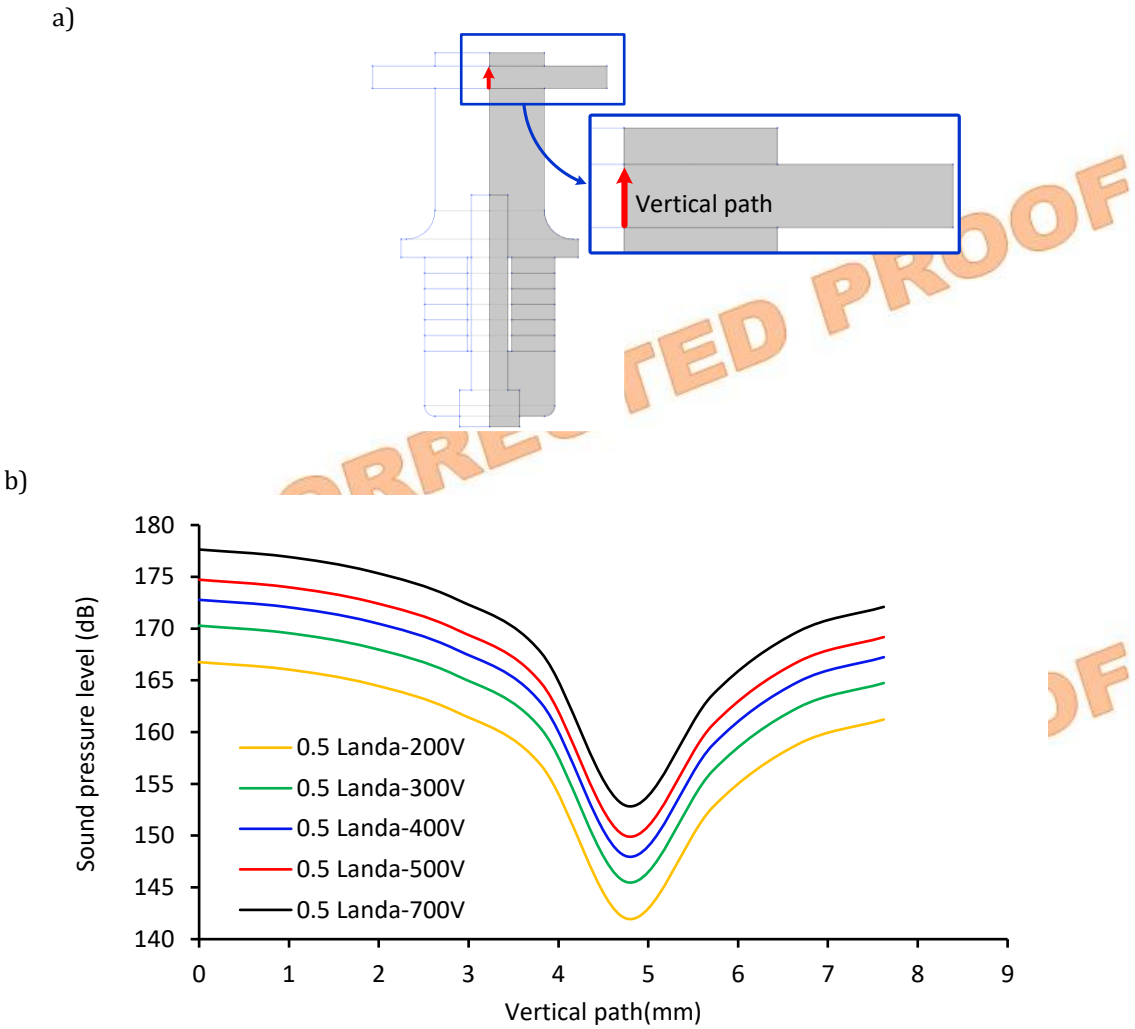

Fig. 8. (a) The vertical path (b)Sound pressure level in λ/2 distance between the transducer and the reflector for different voltage potentials.

A similar trend in the first levitating position at different distances between the transducer and the reflector proves the most stability observed in the highest voltage. Particle movement in the first levitating location in one wavelength between the transducer and the reflector was also studied, and the corresponding model parameters are listed in Table 2. Particle movement trend and corresponding model parameters for a 3λ/2 distance between the transducer and the reflector are presented in Table 3, respectively. Figs. 9 and 10 show the distribution of sound pressure in these situations. It was noticeable from these figures that the best levitating situations in different distances between the transducer and the reflector have a similar sound pressure level. This specific sound pressure level depended upon the mass of a levitated particle.

Table 2. Model parameters for λ distance and selected voltage.

	a	b	c	d	
200V	1686.3326	9694.3332	36.8241	211.2414	Transfer function $\frac{cs+d}{s^2+as+b}$
300V	25.9979	22.4519	-0.1255	0.3325	
400V	7.4268	17.2359	0.0537	0.1889	
500V	473.0081	1.6291	-4.2249	0.0207	
700V	22.2181	84.4719	0.0195	0.5322	

Table 3. Model parameters for 3λ/2 distance and selected voltage.

	a	b	c	d
200V	14.0249	6963.8322	-1.6505	152.9568
300V	39.4131	12.0308	0.6057	0.1753
400V	274.0253	165.9903	1.9385	1.1760
500V	37.6857	33.1876	0.1784	0.2864
700V	53.5574	43.8640	0.3349	0.2750

Transfer function

$$\frac{cs + d}{s^2 + as + b}$$

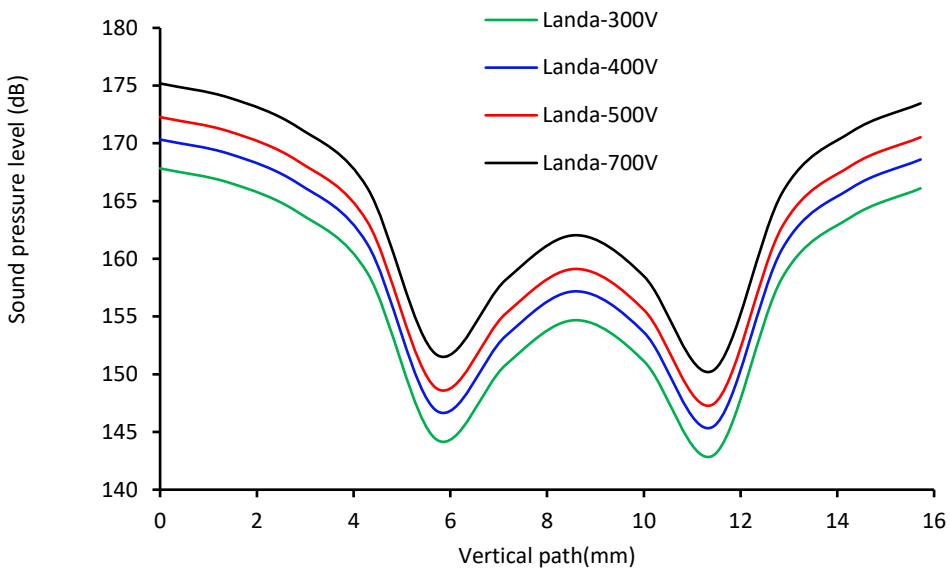

Fig. 9. Sound pressure level in λ distance between the transducer and the reflector in different input voltages.

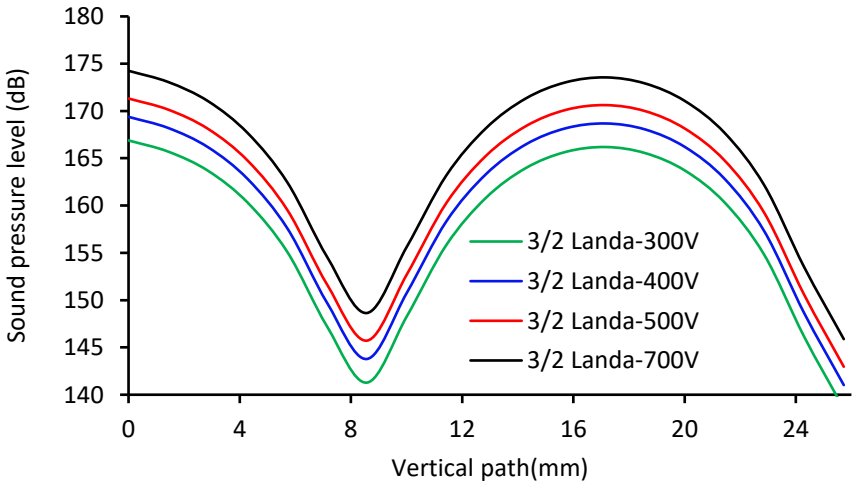

Fig 10. The sound pressure level in the 3λ/2 gap between the transducer and the reflector in different input voltages.

Table 4 shows the effect of the input voltage on the movement of a levitated particle in the second levitating place. The distance between the transducer and the reflector was adjusted to λ. It can be observed that the particle movement trends in the first and second levitating places in a λ wavelength distance between the transducer and the reflector are the same. It can come from a

similarity in pressure distribution. The same trend has been seen for a 3λ/2 gap between the transducer and the reflector. Table 5 shows the trend for a second levitating place in a 3λ/2 distance between the transducer and the reflector. The main difference between the first and second levitating points is the variation between limited voltages in the particle movement trend. Less particle movement of the levitated particle using 700 V comes from more distance between the levitated particle and the transducer. For the 3λ/2 gap, according to Figure 5, the same procedure existed between the second and third levitating locations.

Figure 11 shows the effect of distances between the transducer and the reflector on particle movement in different input voltages for the first levitating location. From this figure, it was seen that in voltages higher than 500 V, more space between the transducer and the reflector led to less particle movement. It happened because more regular pressure distribution existed in more space between the transducer and the reflector. In low voltages, there is no appropriate input acoustic pressure to follow this routine.

Table 4. Model parameters for λ distance and selected voltages.

	a	b	c	d	
200V	0.0001	1.8094	-40.1871	0.1199	Transfer function $\frac{cs+d}{s^2+as+b}$
300V	2758.1155	8401.9226	1.4812	3.9985	
400V	21.4490	14.0304	0.4765	0.4450	
500V	1892.6821	116.7319	-47.9602	-2.4483	
700V	8.2395	1.8682	0.2623	0.0348	

Table 5. Model parameters for λ distance and selected voltages.

	a	b	c	d	
200V	503.3011	702.6611	-18.6506	15.4115	Transfer function $\frac{cs+d}{s^2+as+b}$
300V	84.4753	114.9861	1.2095	1.6802	
400V	10.5053	1.8212	0.0601	0.0200	
500V	20.1498	40.9881	0.2532	0.3588	
700V	1.0863	0.5498	0.0034	0.0034	

Table 6. Model parameters for 3λ/2 distance and selected voltages.

	a	b	c	d	
200V	503.3011	702.6611	-18.6506	15.4115	Transfer function $\frac{cs+d}{s^2+as+b}$
300V	84.4753	114.9861	1.2095	1.6802	
400V	10.5053	1.8212	0.0601	0.0200	
500V	20.1498	40.9881	0.2532	0.3588	
700v	1.0863	0.5498	0.0034	0.0034	

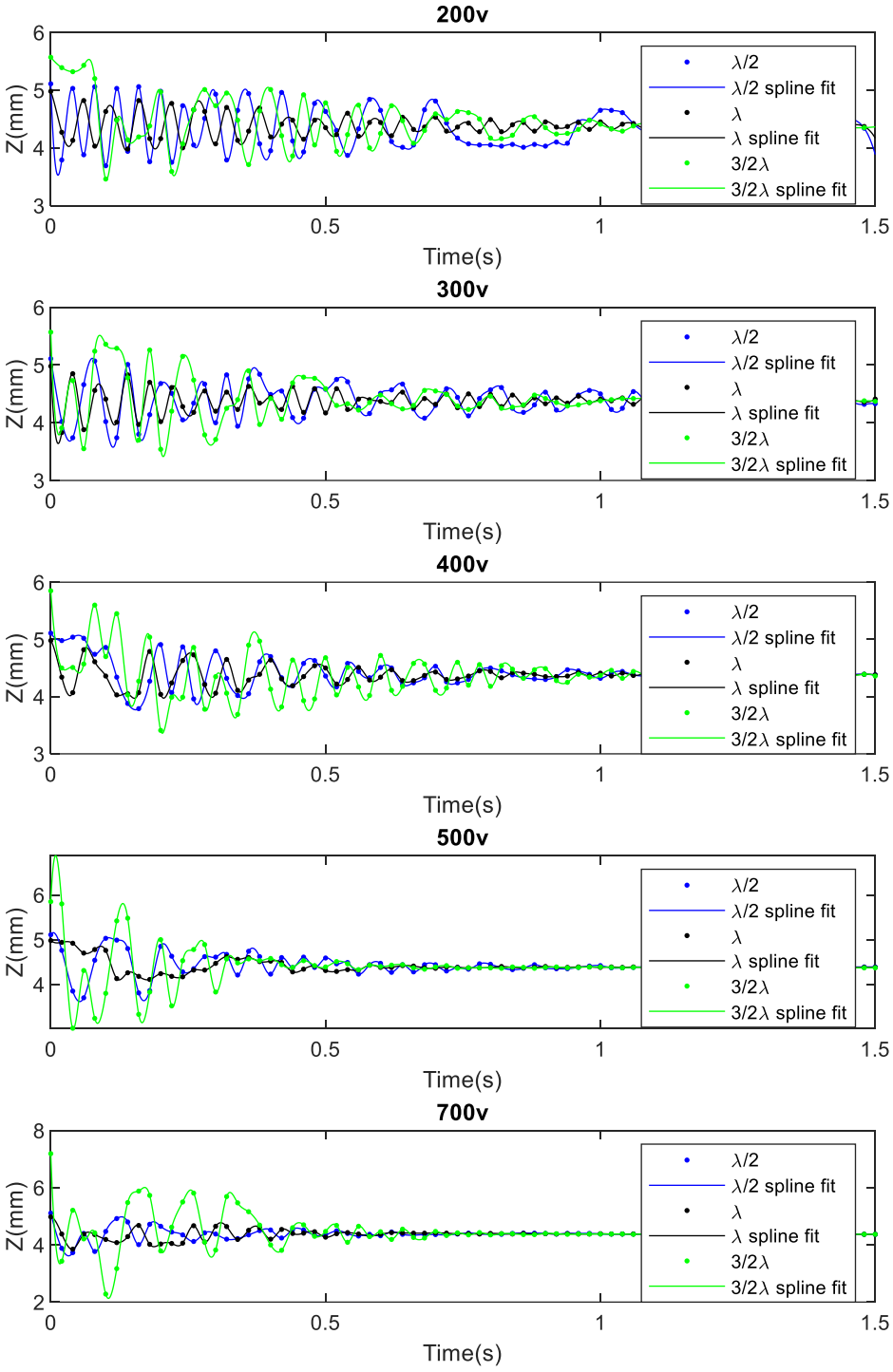

Fig 11. The particle movement in the first levitating location in different distances between the transducer and the reflector for 200V, 300 V, 400 V,500 V, and 700V driving voltages.

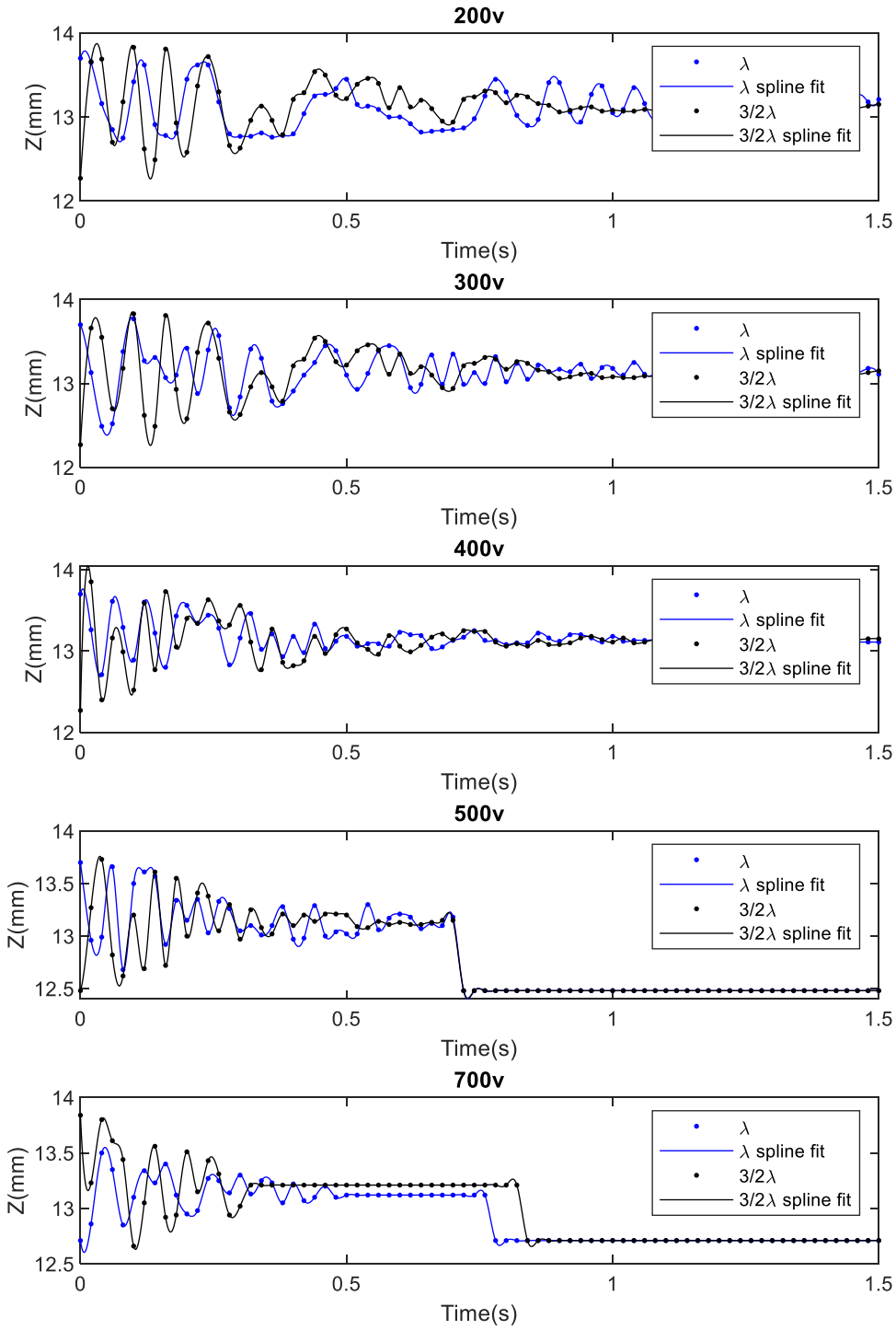

Fig 12. The particle movement in the second levitating location in different distances between the transducer and the reflector for 200V, 300V,400V,500V, and 700V driving voltages.

6. Conclusion

A comprehensive model for the levitated particle movement containing the effect of input voltages and the levitated gap in an ultrasonic levitation process is critical in many applications. For this purpose, numerical simulations were performed to predict the movement of levitated particles in an ultrasonic levitator over a range of selected voltage potentials (200V,300V,400V, 500V, and 700V) and distance parameters between the ultrasonic transducer and the reflector (λ/2, and 3λ/2). Experimental verification of the numerical model shows the

reliability of the simulations. A linear model based on the numerical results for the movement of the particles was derived. The model coefficients were presented in different parameters (voltages and gap). The presented model can be used to control and analyze the levitation.

Funding Statement

This research did not receive any specific grant from funding agencies in the public, commercial, or not-for-profit sectors.

Conflicts of Interest

The author declares that there is no conflict of interest regarding the publication of this article.

Nomenclature

w	Gravity
F_a	ultrasonic force
F_d	drag force
F_b	buoyancy force
r	radius
ρ	density
U	radiation potential
P_p	pressure of particle
v_p	particle velocity
c	ultrasound wave
c	sound speed in levitated medium
c_s	sound speed in levitated particle
Φ_{in}	velocity potential of the acoustic field
m_p	particle mass
τ_p	particle response velocity
v	particle velocity
u	denote fluid velocity
μ	fluid viscosity
ρ_p	particle density
d_p	particle diameter

References

[1] BEAUGNON, E., 1993. Material Processing in High Static Magnetic Field. A Review of an Experimental Study on Levitation. Phase separation and Texturation, 399.

[2] Jayawant, B.V., 1988. Review lecture-electromagnetic suspension and levitation techniques. Proceedings of the Royal Society of London. A. Mathematical and Physical Sciences, 416(1851), pp.245-320.

[3] Ghodsi, M., T. Ueno, and T. Higuchi, Improvement of the magnetic circuit in levitation system using HTS and soft magnetic material. IEEE transactions on magnetics, 2005. 41(10): p. 4003-4005.

[4] Ghodsi, M., Ueno, T. and Higuchi, T., 2005. Improvement of the magnetic circuit in levitation system using HTS and soft magnetic material. IEEE Transactions on Magnetics, 41(10), pp.4003-4005.

[5] Ashkin, A. and Dziedzic, J.M., 1975. Optical levitation of liquid drops by radiation pressure. Science, 187(4181), pp.1073-1075.

[6] Schiffter, H. and Lee, G., 2007. Single-droplet evaporation kinetics and particle formation in an acoustic levitator. Part 1: Evaporation of water microdroplets assessed using boundary-layer and acoustic levitation theories. Journal of pharmaceutical sciences, 96(9), pp.2274-2283.

[7] Bowen, L., 2014. Floating on sound waves with acoustic levitation. COMSOL News, pp.44-45.

[8] Santesson, S. and Nilsson, S., 2004. Airborne chemistry: acoustic levitation in chemical analysis. Analytical and bioanalytical chemistry, 378, pp.1704-1709.

[9] Kremer, J., Bürk, V., Pollak, S., Kilzer, A. and Petermann, M., 2018. Viscosity of squalane under carbon dioxide pressure—Comparison of acoustic levitation with conventional methods. *The Journal of Supercritical Fluids*, *141*, pp.252-259.

[10] Davis, S., Gabai, R. and Bucher, I., 2018. Realization of an automatic, contactless, acoustic levitation motor via degenerate mode excitation and autoresonance. Sensors and Actuators A: Physical, 276, pp.34-42.

[11] Hrka, S., 2015. Acoustic levitation. University of Ljubljana, Faculty of Mathematics and Physics, Ljubljana.

[12] Gor'kov, L.P., 2014. On the forces acting on a small particle in an acoustical field in an ideal

fluid. In Selected Papers of Lev P. Gor'kov (pp. 315-317).

[13] Clift, R., Grace, J.R. and Weber, M.E., 2005. Bubbles, drops, and particles.

[14] Sheykholeslami, M.R., Hojjat, Y., Ghodsi, M. and Cinquemani, S., 2015, March. Comparative discussion between first and second modes of Terfenol-D transducer. In Sensors and Smart Structures Technologies for Civil, Mechanical, and Aerospace Systems 2015 (Vol. 9435, pp. 988-997). SPIE.

[15] Sheykholeslami, M., Hojjat, Y., Ghodsi, M., Kakavand, K. and Cinquemani, S., 2015. Investigation of ΔE effect on vibrational behavior of giant magnetostrictive transducers. Shock and vibration, 2015(1), p.478045.

[16] Sheykholeslami, M., Hojjat, Y., Ansari, S., Cinquemani, S. and Ghodsi, M., 2016, May. Analytical model of a giant magnetostrictive resonance transducer. In Industrial and Commercial Applications of Smart Structures Technologies 2016 (Vol. 9801, pp. 200-206). SPIE.

[17] Sheykholeslami, M., Hojjat, Y., Cinquemani, S., Tarabini, M. and Ghodsi, M., 2016, April. Experimental investigation on dependency of Terfenol-D transducers performance on working conditions. In *Behavior and Mechanics of Multifunctional Materials and Composites 2016* (Vol. 9800, pp. 286-293). SPIE.

[18] Sheykholeslami, M.R., Hojjat, Y., Cinquemani, S., Ghodsi, M. and Karafi, M., 2016. An approach to design and fabrication of resonant giant magnetostrictive transducer. *Smart Structures and Systems*, *17*(2), pp.313-325.Abdullah, A. and A. Pak, Correct prediction of the vibration behavior of a high power ultrasonic transducer by FEM simulation. The international journal of advanced manufacturing technology, 2008. 39(1): p. 21-28.

[19] Abdullah, A., Shahini, M. and Pak, A., 2009. An approach to design a high power piezoelectric ultrasonic transducer. *Journal of Electroceramics*, *22*, pp.369-382.

[20] Hasegawa, K. and Murata, M., 2022. Oscillation dynamics of multiple water droplets levitated in an acoustic field. *Micromachines*, *13*(9), p.1373.

[21] Argyri, S.M., Evenäs, L. and Bordes, R., 2023. Contact-free measurement of surface tension on single droplet using machine learning and acoustic levitation. *Journal of Colloid and Interface Science*, *640*, pp.637-646.

[22] Cancino-Jaque, E., Meneses-Diaz, J., Vargas-Hernández, Y. and Gaete-Garretón, L., 2023. On the dynamics of a big drop in acoustic levitation. *Ultrasonics Sonochemistry*, *101*, p.106705.